Journal of
Polymer Materials

Tech Science Press

https://doi.org/10.32604/jpm.2026.077511

ARTICLE

Development of *Calopogonium mucunoides* PEGylated Solidified Reverse Micellar Suspensions: Polymer-Matrix Design for Sustainable Wound Application

Edith O. Diovu[1], Calister E. Ugwu[2,*], Eunice N. Anaele[3,*], Samuel WisdomofGod Uzondu[4], Ogochukwu N. Umeh[2], Iheanacho O. Enyum[2], Kingsley C. Eze[2], Godswill C. Onunkwo[2] and Anthony A. Attama[5]

[1]Department of Pharmacognosy and Environmental Medicine, Faculty of Pharmaceutical Sciences, University of Nigeria, Nsukka, Nigeria
[2]Department of Pharmaceutical Technology and Industrial Pharmacy, Faculty of Pharmaceutical Sciences, University of Nigeria, Nsukka, Nigeria
[3]South-East Zonal Biotechnology Centre/Department of Microbiology, University of Nigeria, Nsukka, Nigeria
[4]Nanosciences and Advanced Materials Programme, Federal University of ABC, Santo Andre, SP, Brazil
[5]Department of Pharmaceutics, Faculty of Pharmaceutical Sciences, University of Nigeria, Nsukka, Nigeria

*Corresponding Authors: Calister E. Ugwu. Email: calister.ugwu@unn.edu.ng; Eunice N. Anaele. Email: ngozi.anaele@unn.edu.ng

Received: 10 December 2025; Accepted: 27 April 2026; Published: 30 June 2026

ABSTRACT: Polymer-lipid hybrid-based solidified reverse micellar suspensions (SRMs) have gained increasing interest for topical drug delivery due to their ability to enhance solubility, stabilize bioactive compounds, and achieve sustained skin permeation. In this study, PEGylated SRMs were developed using a beeswax: Phospholipon 90H lipid matrix to enhance the solubility, stability, bioavailability, and wound-healing properties of a lipophilic extract of *Calopogonium mucunoides* (CM). PEG: lipid matrix ratios (1:0, 0:1, 1:1, 1:2, 1:3) were formulated and designated as CM1–CM5, with an unloaded matrix (CM6) as control. Physicochemical characterization included encapsulation efficiency (EE%), spreadability, pH, viscosity, Fourier transform infrared spectroscopy (FTIR), differential scanning calorimetry (DSC), scanning electron microscopy (SEM), and dynamic light scattering (DLS). *In vitro* release and excision wound-healing assays were also conducted. PEGylated CM.SRMs demonstrated tunable polymer-matrix interactions influencing drug loading and release behavior. The CM5, with the highest lipid content, showed maximum EE (77%) and optimal rheological properties for skin retention. FTIR and DSC confirmed successful molecular dispersion of CM within the polymer-lipid matrix without chemical incompatibility. SEM revealed rough and porous structures that supported prolonged and sustained release, with particle sizes in the nanoscale (27.02 nm), and release rates ranging from 48% to 90% over 6 h, depending on the PEG: lipid ratio. *In vivo*, CM.SRMs achieved significantly accelerated wound contraction (~99%) and enhanced epithelialization compared to the standard treatment ($p < 0.05$). These findings demonstrate that PEGylated polymer-lipid SRMs can improve bioavailability and provide sustained therapeutic action of phytochemicals at the wound site. This polymer-engineered delivery system offers a promising, sustainable alternative for wound management, particularly in resource-limited settings. However, the histological and other biomarkers-based validation are recommended.

KEYWORDS: *Calopogonium mucunoides*; solidified reverse micellar suspensions; PEGylation; wound healing; beeswax; polymer-lipid matrix

1 Introduction

Chronic wounds affect millions of people worldwide, with an estimated 25% of individuals experiencing them annually [1], making them a major global healthcare and economic burden. The global wound care market is projected to exceed 29.6 billion USD by 2030 [2]. Chronic wounds typically arise from injuries to the skin and underlying tissues, including diabetic foot ulcers, pressure sores, and venous leg ulcers, which fail to heal within the normal timeframe and often persist for weeks or months [3]. Despite improved scientific understanding of the biological processes involved in wound healing, conventional treatments such as topical medications and wound dressings frequently provide inadequate management for severe wounds [4]. Consequently, there is an urgent need for innovative therapeutic strategies capable of enhancing tissue regeneration and improving wound repair outcomes. Herbal remedies derived from plants have attracted considerable attention in healthcare management owing to the presence of diverse bioactive compounds (BCs) that function as secondary metabolites in plants [5,6]. In addition, plant-based therapeutics are widely accessible, often require minimal industrial processing, and are generally economically sustainable and cost-effective. Several studies have demonstrated that plant phytoconstituents such as alkaloids, flavonoids, terpenes, and carbohydrates can promote wound healing by stimulating cellular regeneration and tissue repair processes [5,7].

Among these medicinal plants, *Calopogonium mucunoides* (CM), commonly known as wild groundnut, has been widely used in traditional medicine to treat skin injuries such as cuts and wounds due to its lipophilic phytoconstituents with antimicrobial, anti-inflammatory, and antioxidant properties [8]. CM contains several phytoconstituents, including alkaloids, terpenoids, glycosides, flavonoids, phenols, and quinones, which are believed to contribute to its pharmacological activities. Furthermore, ethanolic extracts of CM have been reported to exhibit strong anti-inflammatory activity by reducing platelet aggregation, phospholipase-A2 activity, albumin denaturation, and hypotonicity-induced haemolysis in a concentration-dependent manner [9]. In another study evaluating the anti-ulcer potential of CM, treatment produced a gastric cytoprotective effect, significantly reducing ulcer index, gastric juice secretion, and free and total acidity compared with the control group [10]. These pharmacological properties suggest that CM contains biologically active phytochemicals with potential therapeutic value for tissue repair and inflammatory skin conditions.

Despite its promising therapeutic potential, the utilization of CM for dermal applications remains limited by several challenges. Most of its bioactive phytoconstituents are lipophilic, which complicates their effective delivery across the skin barrier [8]. The skin's protective outer layer, the stratum corneum, consists of tightly packed keratinocytes embedded within intercellular lipids such as cholesterol, fatty acids, and saturated lipids. This forms a highly efficient biological barrier that restricts the penetration of therapeutic agents [11]. In addition, lipophilic bioactive compounds often exhibit poor aqueous solubility, limited dermal permeability, relatively large molecular size, and susceptibility to metabolic degradation, all of which reduce their therapeutic effectiveness [12]. These limitations highlight the need for advanced drug-delivery systems capable of improving the solubility, stability, and dermal transport of plant-derived bioactive compounds.

Lipid-based delivery systems have gained significant attention for the dermal delivery of lipophilic bioactive compounds owing to their ability to improve solubility, enhance physicochemical stability, facilitate dermal penetration, and provide controlled drug release [13]. Such systems can also protect phytochemicals from degradation while improving their bioavailability and therapeutic performance [14]. Among the various lipid-based technologies, solidified reverse micellar suspensions (SRMs) represent an emerging polymer-lipid hybrid platform that integrates the structural advantages of reverse micelles with the stability of a solid lipid matrix. This hybrid architecture enables the encapsulation of both hydrophilic and lipophilic

compounds while allowing tunable polymer–matrix interactions that influence drug loading, matrix organization, and release kinetics [15]. PEGylation further enhances the physicochemical performance of SRMs by modulating matrix hydration, improving spreadability, and increasing drug diffusion across biological barriers through polymer chain mobility and surface interactions [16]. In recent decades, various advanced topical delivery systems, such as hydrogels, liposomes, nanoparticles, and nanofiber-based scaffolds, have been developed to enhance wound healing outcomes. However, these systems often exhibit limitations such as poor stability, rapid drug leakage, limited retention at the wound site, and insufficient control over drug release within the dynamic wound microenvironment [17]. In contrast, PEGylated-lipid matrix offers improved structural flexibility, enhanced hydration, reduced aggregation, and more sustained and controlled release, thereby improving drug stability and retention at the site of application [16].

Despite the increasing interest in lipid-based delivery systems for plant-derived therapeutics, the application of PEGylated SRM systems for the topical delivery of *Calopogonium mucunoides* phytochemicals has not been previously reported. Therefore, this study aimed to develop PEGylated solidified reverse micellar suspensions incorporating the lipophilic extract of *Calopogonium mucunoides* using a beeswax-Phospholipon® 90H (Bw: P90H) lipid matrix. We hypothesized that encapsulating CM within a PEGylated polymer-lipid SRM platform would enhance the solubility, stability, dermal bioavailability, and sustained release of its bioactive compounds.

The formulations were optimized by systematically investigating the influence of PEG-lipid matrix ratios on encapsulation efficiency, physicochemical characteristics, and drug-release behavior. Structural and physicochemical analyses were performed to evaluate polymer-matrix interactions and their influence on drug loading and release kinetics. Finally, the wound-healing potential of the optimized CM-loaded SRM formulations was evaluated using an *in vivo* excision wound model, providing preliminary evidence for their potential application as a polymer-lipid hybrid delivery platform for plant-based wound therapeutics.

2 Materials and Methods

2.1 Materials

The following materials were employed in the research: Phospholipon 90H (Phospholipid GmbH, Köln, Germany), propylparaben (Quolikems, India), glycerin (CDH-Central Drug Howe, India), PEG 6000 (Sigma Aldrich, USA), n-hexane (Emsure, Germany). Dialysis membrane (MWCO 8000–10,000, Spectrum Labs, The Netherlands), Cicatrin (Glaxo, UK), Albino rats [Department of Veterinary Medicine, University of Nigeria, Nsukka (UNN)]. Beeswax (procured from Opi Market, Nsukka) and the whole herb of *Calopogonium mucunoides* harvested from the UNN farm and was authenticated by a taxonomist at the Herbarium section (No. UNN/13054) of the Department of Pharmacognosy and Environmental Medicine, and both processed and extracted in the Pharmaceutical Technology laboratory, UNN. The other reagents were of analytical quality grades.

2.2 Extraction of Calopogonium mucunoides Oil

The oil component of *Calopogonium mucunoides* (CM) was extracted using the Soxhlet extraction technique by a previous technique, with a little modification [18]. In brief, about 680 g of dried whole herb of *Calopogonium mucunoides* was pulverized to a powdered form using a milling machine (500# grinder/Fuyu metal, LinyiFuyu metals product Co., Ltd., China). The powdered sample was weighed (170 g) and extracted using a Soxhlet apparatus with 750 mL of n-hexane for about 4 h at 25°C. This solvent was selected to preferentially recover the lipophilic constituents of the plant. The resulting filtrate was condensed with a Rotary evaporator (Heidolph Instruments GmbH and Co., KG, Schwabach, Germany) and air-dried to allow

complete evaporation of the solvent. Thereafter, the dried extract and percentage yields were determined using Eqs. (1) and (2).

$$Extract\ yield = \frac{Amount\ of\ extract\ produced}{\text{Amount of powdered plant used for extraction}} \quad (1)$$

$$Percent\ extract\ yield = Extract\ yield \times 100 \quad (2)$$

2.3 Qualitative and Quantitative Phytochemical Analysis

CM was standardized based on its total extract concentration using UV-Vis spectrophotometry (Jenway 6705, USA). A calibration curve (Beer-Lambert plot) was generated using serial dilutions of the n-hexane extract and absorbance measured at 218 nm (predetermined). The experimental conditions and calibration curve are provided in the Supplementary Data. Phytochemical screening of CM was performed to identify the major phytoconstituents present in the extract according to previously described methods [18].

2.4 Preparation of Calopogonium mucunoides-Based Solid Reverse Micellar Suspensions (CM.SRMs)

2.4.1 Purification of Beeswax

Approximately 200 g of Beeswax (natural fat) was extracted from natural honey combs and then melted and purified by incorporating 2% suspension of charcoal and bentonite in a 1:9 ratio, mixed into the melted beeswax at 60°C–70°C in a thermoregulated water bath. Then, vacuum-filtered with a Buchner funnel to obtain pure beeswax.

2.4.2 Preparation of Lipid Matrix, PEGylation, and Drug Loading of SRMs

Lipid matrix was prepared using the fusion method with little modifications according to Ugwu et al. [16]. Briefly, the lipid matrix of beeswax (Bx) and Phospholipon 90H (P90H) were prepared at a Bx: P90H ratio of 0.5:4.5 (g w/w). Appropriate amounts of Bx: P90H were weighed, mixed, melted, and stirred in a thermoregulated water bath at a temperature between 60°C–70°C until a homogenous admix was obtained. The molten mixture was stirred thoroughly until it solidified to obtain the solidified reverse micellar suspensions (SRMs). Thereafter, appropriate quantities of polyethylene glycol (PEG 6000) and the lipid matrix (Bx: P90H) were melted together at the same temperature in various ratios of 1:0, 0:1, 1:1, 1:2, 1:2, and 1:3 and then, loaded with approximately 200 mg CM to get 5 g PEGylated SRMs producing six preparations CM1, CM2, CM3, CM4, CM5, respectively, and additional PEG: lipid matrix 1: 2 (CM6), which was prepared without drug loading (unloaded) and served as a placebo, using a cold high shear homogenization method. Simultaneously, a 3 g weight of the surfactant (glycerin) and 0.5 g of the preservative (propylparaben) was weighed into a 100 mL beaker and mixed evenly until a homogenous mix was obtained and incorporated into each lipid matrix and volume adjusted to 100 mL with 30% ethanol and then, homogenized (Ultra-Turrax T18, Basic, Ika, Germany) at 10,000 rpm for 5 min to obtained a drug loaded PEGylated SRMs denoted as CM1–CM5 (drug loaded) and CM6 (unloaded). The resulting SRMs were put in airtight containers and stored in a cool, dry place until further evaluations. The composition formula for the preparation is in the Supplementary Table S1.

2.5 Characterization of Calopogonium mucunoides-SRMs (CM.SRMs)

2.5.1 Determination of Encapsulation Efficiency and Loading Capacity

Encapsulation efficiency (EE) and Loading capacity (LC) were determined using an ultrafiltration-centrifugation method [16]. Briefly, a microconcentrator (5000 MWCO Vivascience, Hanover, Germany) was filled with approximately 5 mL of each CM.SRMs. After centrifuging the microconcentrator (TDL-4

B. Bran Scientific and Instrument Co., London, England) for two hours at 4000 rpm, the supernatant was collected and diluted with n-hexane, then concentrated HCl was added, and the mixture was heated at 60°C for 30 min in triplicate. The drug concentration was sufficiently assessed using spectrophotometry (Jenway 6705, USA) at a preset wavelength (218 nm). Eq. (3) was used to compute the quantity of CM encapsulated in the SRMs with reference to the Beer-Lambert plot of CM (Supplementary Fig. S1) as obtained from Table S2 to determine the EE%.

$$EE\,(\%) = \frac{Initial\ amount\ of\ drug - Amount\ of\ drug\ in\ supernatant}{\text{Initial amount of drug}} \times 100 \tag{3}$$

2.5.2 Physicochemical Characterization of CM.SRMs

Determination of the Spreadability Index, pH, and Viscosity

Spreadability, pH, and viscosity of CM-SRMs were assessed using standard methods [19]. Spreadability of the CM.SRMs was evaluated using a simple glass slide compression (100 g, 3 min) and expressed as the spreadability index (SI). Briefly, a volume of 0.5 mL of each formulation was accurately measured using a syringe and placed at the centre of a clean, dry glass slide premarked to be 1.0 cm in diameter. A second glass slide of the same dimensions was gently lowered onto the first, allowing the formulation to spread naturally between the two slides without any applied pressure. To ensure uniform spreading, a 100 g weight was carefully placed on top of the upper slide and left in position for about 3 min, to enable an even distribution into a thin film. Thereafter, the weight was removed, and the diameter of the resulting spread was measured using a standard ruler. The test was repeated in triplicate. The SI was determined using Eq. (4).

The pH was measured potentiometrically in a timed manner at 25°C 1, 8-, and 15-weeks post-formulation. Briefly, the electrode of the pH meter (Hanna Instrument, Romania) was inserted into each formulation in triplicate, and the mean pH value recorded after calibration with standard buffer.

The viscosity was measured using a digital viscometer (NDJ-5S Viscometer, Labscinces, England), with a specific spindle (#04) at the speeds of 60 rpm and 25°C. In brief, the spindle was immersed in the sample placed in a sizeable beaker and attached to the coupling nut such that the formulation level was at the groove on the shaft, and then, the viscosity recorded.

$$SI\,(\%) = \frac{ID\,(cm)}{D\,(cm)} \tag{4}$$

where *SI* (spreadability index); *ID* (increase in diameter); and *D* (initial diameter).

Fourier Transform Infrared Spectroscopy (FTIR)

The FTIR spectroscopy for the CM, beeswax, Phospholipon 90H, PEG 6000, glycerin, and selected *Calopogonium mucunoides*-based SRMs (CM4) (containing PEG: lipid matrix 1:2) and unloaded CM6 (containing PEG: lipid matrix 1:2) was recorded using an infrared spectrophotometer (IRAffinity-1, Shimadzu FTIR-8400, Germany) according to an earlier method [16]. The samples were prepared in a KBr disk (2 mg sample/200 mg KBr) with a hydrostatic force of 275,790.292 Pa for 4 min, and the background spectrum was obtained under similar conditions. Spectra were determined from single mean scans obtained in the region within 4000–400 cm^{-1} with a spectral resolution of 2 cm^{-1} and ratio against the background interferogram.

Differential Scanning Calorimetry (DSC)

DSC analysis was carried out on the CM, excipients (beeswax, phospholipon 90H, polyethylene glycol, and glycerin), and loaded and unloaded CM.SRMs using DSC equipment (Netzsch DSC 204 F1, Geratebau, GmbH, Selb, Germany) according to a previous method with little modification [16]. In brief, the thermograms of the samples were analyzed by measuring about 4 mg of each sample inside an aluminum

crucible to obtain the thermal characteristics within the range of 20°C–400°C with heat at 10 K/min under a nitrogen flux (20 mL/min).

Scanning Electron Microscopy (SEM) and Particle Size Analysis

The SEM and morphology of CM, glycerin, beeswax, and loaded and unloaded CM.SRMs (CM4 and CM6 containing PEG: LM 1:2) were carried out using computerized image analysis with a photo microscope. A 2 mg sample of the extract was dispersed in a small amount of distilled water on a microscope slide, covered with a coverslip, and examined under a light microscope. The diameter of the particles, representing the extract's particle size, was measured at a magnification of ×400. The morphology of the particles was observed and documented using a scanning electron microscopy (SEM) (JEOL-JSM-6360, Japan). A drop of each prepared sample was placed on a slide and allowed to dry at ambient temperature, and then placed on a specimen holder with double-coated adhesive tape and gold coating under vacuum using a sputter coater (Model JFC-1100, JEOL, Japan) for 10 min, and then investigated at 20 kV.

Particle size distribution of the pure *Calopogonium mucunoides* extract and selected PEGylated SRM formulation (CM, PEG: lipid matrix 1:2) were determined using dynamic light scattering (DLS) (Malvern Zetasizer, Malvern Instruments, UK). Samples were dispersed in distilled water and measured at 25°C using disposable cuvettes. Each measurement was performed in triplicate, and the results were reported as mean values.

2.6 In Vitro Study and Release Kinetics of CM.SRMs

The *in vitro* release of CM from CM.SRMs study was investigated using the dialysis bag technique as earlier described [17]. Approximately 10 mg of the loaded CM.SRMs was incorporated in about 4 cm length polycarbonate dialysis bag (~6000–8000 Da; MWCO 8000–10,000) immersed in a beaker containing 200 mL medium of simulated acidic fluid (SAF, pH 1.2) assembled on a magnetic stir maintained with gentle stirring at approximately 100 rpm to ensure uniform mixing and temperature of 37 ± 0.5°C. This was conducted for over a period of 2 h, during which 2 mL samples were withdrawn at predetermined time intervals (15, 30, 60, 90, and 120 min), and replaced with the same volume of fresh SAF. After the 2-h exposure in SAF, the dialysis bag was carefully removed, rinsed gently with distilled water to eliminate residual SAF, and transferred to a new beaker containing 200 mL of simulated wound microenvironment fluid (SMF, pH 6.8) to simulated wound microenvironment and sampled at regular intervals of 30 min for a period of 4 h under similar conditions. All collected samples were subsequently analyzed in triplicate for CM content using UV-Vis spectrophotometry (Jenway 6705, USA), and the cumulative percentage CM released was calculated and plotted as a function of time. Then, to elucidate the release mechanism of CM from the SRM formulations, the release data obtained from the SAF and SMF were fitted into different kinetic models, including zero-order, first-order, Higuchi, and Korsmeyer-Peppas equations. The goodness of fit of each model was evaluated using the correlation coefficient (R^2), and the model with the highest R^2 value was considered to best describe the release behavior. For the Korsmeyer-Peppas model, the release exponent (n) was used to further characterize the transport medium.

2.7 In Vivo Study

2.7.1 Ethical Approval

Experimental animal protocols were conducted according to the guidelines for conducting experiments stipulated and approved by our Institution's Animal Ethics Committee of Faculty of Pharmaceutical Sciences Research Ethics (approval No. FPSRE/UNN/25/00044) and in compliance with the Federation of European Laboratory Animal Science Associations and the European Union Directive 2010/63/EU for animal experiments.

2.7.2 Experimental Animals

The wound healing property of CM.SRMs were investigated using the excision wound model technique reported earlier, with little modification [20]. The experimental animals used were procured from the Department of Veterinary Medicine, University of Nigeria, Nsukka (UNN). They were made of twenty-four healthy Albino rats of both sexes, weighing within 120–150 g. The Albino rats were housed in stainless steel cages maintained at 25°C with a 12-h light/dark cycle, as well as on a normal diet of commercial livestock feed and with unlimited access to water. They were divided into four groups of six each. The groupings for topical treatment include: Group A—received 5 mg/Kg CM.SRMs (CM5); Group B—received 5 mg/kg Cicatrin powder (standard reference); Group C—received 5 mg/kg unloaded SRMs (placebo); Group D—received no treatment (Control group). The rats were anaesthetized prior to creation of the wound, with 1 mL of intravenous ketamine hydrochloride (10 mg/kg body weight). The dorsal fur of each animal was shaved with an electric clipper, and the area where the wound would be created was outlined on the back of the animal with ink. A fully thick excision wound (2 cm diameter) was created along the markings using a toothed forceps and pointed scissors.

For all the treated cases, the appropriate formulation was applied to the wound immediately after wounding. The measurement of the wound areas was taken on the 3rd, 7th, 14th, and 21st day following the initial wound with the aid of a transparent ruler. The wound size contraction was calculated using Eq. (5).

$$\%WC = \frac{HWS}{\mathrm{TWS}} \times 100 \tag{5}$$

where *WC* (wound contraction), *HWS* (healed wound size), and *TWS* (total wound size).

2.8 Statistical Analysis

Results were expressed as mean ± SD. Physicochemical measurements were performed in triplicate unless otherwise stated. One-way ANOVA with Tukey's post-hoc test assessed significance at $p < 0.05$.

3 Results and Discussion

3.1 Phytochemical Compounds and % Yield

CM-loaded PEGylated solidified reverse micellar suspensions (CM-SRMs) were developed using the homogenization approach to enhance the incorporation and topical delivery of lipophilic *Calopogonium mucunoides* extract. The system was designed based on a polymer-lipid matrix concept with beeswax and Phospholipon® 90H constituting the lipid phase and polyethylene glycol (PEG 6000) serving as the hydrophobic polymer component. The types and ratios of these excipients were carefully selected to optimize encapsulation efficiency, structural stability and topical applicability. Given the lipophilic nature of CM, incorporation into a lipid-rich matrix was essential to improve its solubilization and retention within the formulation. Hydrophobic matrices are known to enhance the loading of lipophilic phytoconstituents in topical delivery systems because they provide a chemically compatible environment that maximizes solubility and entrapment. These systems have been shown to overcome low aqueous solubility and poor membrane permeability common with many plant-derived compounds [21]. Beeswax was incorporated as a solid lipid to provide structural rigidity and promote formation of a stable matrix, while Phospholipon® 90H provided amphiphilic characteristics that facilitated interfacial stabilization and improved compatibility between hydrophilic and hydrophobic components. PEG 6000 was introduced to modulate hydration, reduce interfacial tension and enhance spreadability. PEGylation has been widely reported to improve formulation stability and surface characteristics in topical and colloidal systems [21]. By varying the PEG-to-lipid matrix ratio (CM1-CM5), a series of formulations was generated to systematically evaluate the influence of polymer-lipid interactions on formulation performance.

The process involved several steps. First, the lipophilic CM bioactive compounds were extracted with n-hexane using the Soxhlet extractor apparatus. Phytochemical analysis of the CM revealed the presence of several phytochemicals including flavonoids, tannins, phenolics, alkaloids, saponins, terpenoids, and soluble carbohydrates, with saponin exhibiting the highest concentration of 8.35 ± 0.07 mg/100 g (Fig. 1A). The presence of these phytochemicals is particularly important as several of them have been reported to contribute to the wound healing process. For example, flavonoids and phenolic compounds possess strong antioxidant and anti-inflammatory properties, which can mitigate oxidative stress and promote wound healing [22]. Saponins and terpenoids have been associated with antimicrobial activity and enhancement of collagen synthesis [23]. All these contribute to the wound healing cascade and therefore support the potential therapeutic relevance of CM for topical wound management. Next, the lipid excipients were melted in their respective ratios and stirred gently at 60°C–70°C, followed by incorporation of a small quantity of CM in the molten matrix. The mixture was subsequently homogenized to form a uniform dispersion and thereafter controlled cooling to allow solidification of the lipid phase to form a structured reverse micellar matrix. The resulting CM-SRMs formed visually homogeneous, semi-solid systems, indicating successful incorporation of the extract within the polymer-lipid matrix. Blank formulations prepared without CM displayed similar structural characteristics, confirming that the system architecture was primarily governed by the excipient composition. This formulation strategy intends to overcome the inherent limitations associated with the lipophilicity of CM and to enable controlled topical delivery.

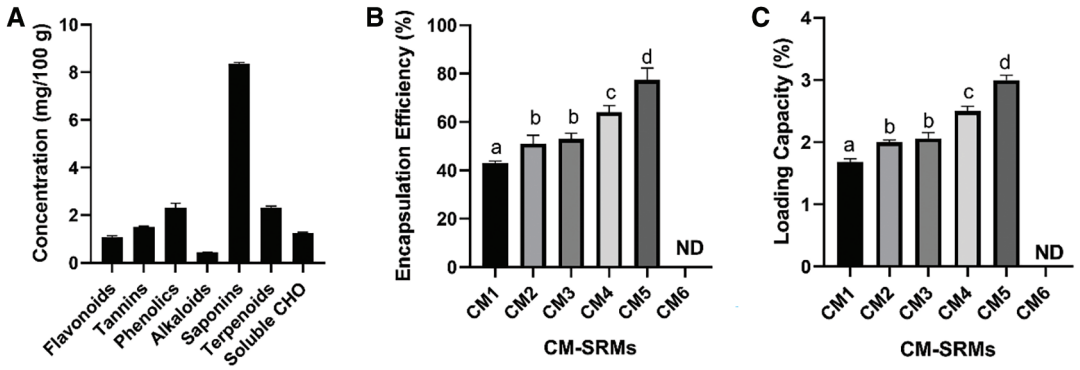

Figure 1: Characterization of CM and CM-SRMs (**A**) quantitative phytochemical evaluation of CM (**B**), encapsulation efficiency (%) of CM-SRMs, and (**C**) loading capacity (%) of CM-SRMs. Data are presented as mean ± SD (n = 3). Bars with different letters indicate statistically significant differences ($p < 0.05$), ND: not detected. CM1: PEG only (1:0); CM2, CM3, CM4, and CM5 correspond to PEG: lipid matrix (LM) ratios of 0:1, 1:1, 1:2, and 1:3, respectively, while CM6 is the blank formulation without drug.

In the % yield, 170 g of the dried milled crude sample after extraction yielded 2.7 g oil extract of CM with a percentage yield of 1.59%. The low % yield may be a result of any of these factors, such as the nature of the required constituents of the sample, transfer losses, nature and concentration of solvent, level of particle size reduction, amount of the materials used, solvent: material ratio, and others. This is in agreement with an earlier report [9].

3.2 Encapsulation Efficiency of CM-Loaded SRMs

Encapsulation efficiency (EE%) helps to ascertain the amount of drug loaded in a formulation that was entrapped. The EE (%) and LC are key parameters in lipid-based delivery systems. They reflect the ability of the carrier matrix to incorporate and retain bioactive compounds [24]. High EE is particularly important for topical delivery, as it ensures sufficient drug availability at the site of application while minimizing loss and

enhancing formulation stability [25]. Lipid-based systems are especially suited for lipophilic compounds due to their affinity for hydrophobic domains, where the lipid matrix acts as a reservoir for sustained release and improved skin retention [26].

The EE% of the CM.SRMs, as shown in Fig. 1B, ranged within 42%–77% with CM5 (PEG: LM ratio 1:3) exhibiting the highest EE (77%) and CM1 (PEG: LM ratio 1:0) the lowest EE%. PEGylated formulations demonstrated notable variation in EE% depending on polymer–lipid ratios. Increasing the lipid content improved EE%, likely due to enhanced solubilization and retention of lipophilic CM within the beeswax-rich matrix. PEG-only CM1 displayed the lowest EE%, confirming the essential role of a hydrophobic domain for efficient drug loading. The overall increase in EE with higher lipid content can be attributed to improved solubilization and partitioning of the lipophilic extract within beeswax-phospholipid matrix, which provides a compatible hydrophobic environment for extract incorporation [27]. In contrast, the PEG-only formulation showed limited encapsulation, highlighting the importance of a lipid core for efficient loading. These findings demonstrate that polymer-lipid composition plays a critical role in modulating encapsulation performance in SRM systems. Extract loading ranged from 1.68% to 3.0%, with CM5 exhibiting the highest loading capacity, consistent with its superior encapsulation efficiency (Fig. 1C). The relatively low LC values are typical for lipid-based systems incorporating crude extracts [18]. LC showed a similar trend with EE, with significant differences observed across most formulations ($p < 0.05$), except for CM2 and CM3. This is expected as LC is directly dependent on EE and further confirms the internal consistency and reliability of the formulation system.

3.3 Physicochemical Properties of CM-Loaded SRMs

3.3.1 Spreadability Index, pH, and Viscosity

To evaluate the physicochemical characteristics and stability of the CM-loaded SRMs, key parameters including spreadability, pH, and viscosity were assessed across the different polymer-lipid compositions. These properties are critical for topical delivery systems, as they influence formulation stability, drug release, and skin retention [28]. PEG incorporation improved hydration, spreadability, pH uniformity, and rheological behavior across formulations, enhancing dermal compatibility.

The spreadability index is a crucial property of a topical application, indicating the area the formulation can reach after application. The viscosity of the formulation is influencing it. It has an inverse relationship with the viscosity. The spreadability index (SI) of CM.SRMs as presented in Fig. 2A ranged within 10.6 to 11.8 cm^2/s. The CM1 (containing PEG: LM in a 1:0 ratio) exhibited the highest SI (11.8 cm^2/s) due to the less viscous property of PEG in the absence of lipid matrix (LM). This indicated that the absence of LM leads to lower viscosity, allowing the formulation to spread more easily. This was followed by an unloaded CM6 formulation with a relatively high SI (11.2 cm^2/s), due to the absence of the drug. The SRMs containing LM and CM (CM3, CM4, and CM5) showed slightly lower SI (insignificant) with an enhanced fluid consistency, ranging from 10.6 to 10.8, which decreased with a decrease in lipid matrix content. Formulations CM3 and CM4 (SRMs containing PEG: LM 1:1 and 1:2) had identical SI values (10.6 cm^2/s), suggesting that the SRMs at these ratios slightly increased viscosity, which in turn reduced spreadability. Formulation CM5 (containing PEG: LM 1:3) exhibited the least SI (10.4 cm^2/s), resulting in a slightly more spreadable product. The presence of CM slightly reduced the spreadability compared to the unloaded base. This is beneficial as a slightly more viscous formulation can improve skin retention time and reduce runoff after application. Thus, the CM.SRMs maintain adequate spreadability for topical use. Despite these differences, all formulations demonstrated good overall spreadability, with SI values above 10 cm^2/s, which indicates suitability for topical application [19].

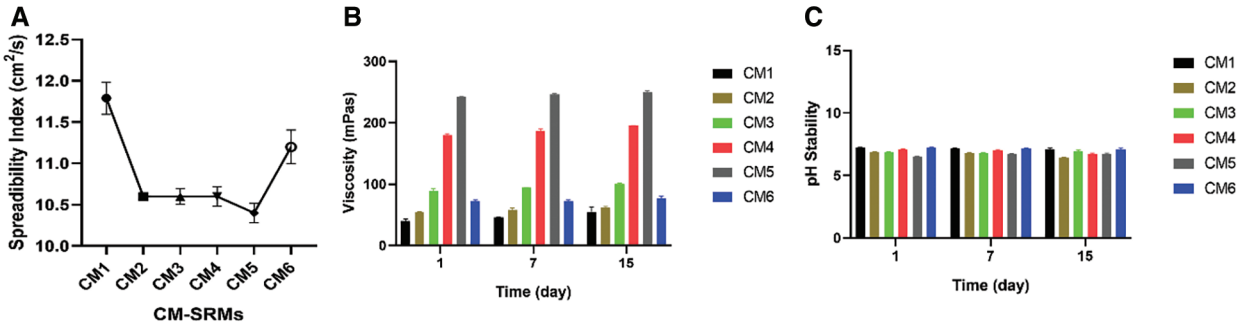

Figure 2: Physicochemical characterization of CM-SRMs (**A**) spreadability index (SI) of CM-SRMs, (**B**) effect of formulation composition and storage time on viscosity of CM-SRMs, (**C**) pH of CM-loaded SRMs during storage. Data are presented as mean ± SD (n = 3). Statistical analysis was performed using two-way ANOVA followed by Tukey's multiple comparisons test ($p < 0.05$). CM1: PEG only (1:0); CM2, CM3, CM4, and CM5 correspond to PEG: lipid matrix (LM) ratios of 0:1, 1:1, 1:2, and 1:3, respectively, while CM6 is the blank formulation without drug.

Viscosity is an important parameter to consider in topical preparation as it influences drug release profile, stability, spreadability, and pourability. Viscosity was significantly influenced by both formulation composition and storage time, with formulation effects being more pronounced. The inverse relationship between viscosity and spreadability reflects increased structural organization within lipid-rich formulations, which limits flow but enhances matrix integrity. It is an important trend regarding the physical stability of the formulations over time. The viscosity results of the SRMs, as presented in Fig. 2B, ranged within 42–242 mPas. All formulations demonstrated a gradual increase in viscosity from Day 1 to Day 15, suggesting progressive structural rearrangement within the matrix. Formulation with a higher lipid matrix exhibited higher viscosity as observed in the CM5 formulation (250 mPas). The viscosity stability study provides valuable insights into the rheological behaviors of these SRMs, while the least viscosity was observed in the formulation containing PEG (CM1) only. An earlier report has shown that PEGylation reduces resistance to flow by reducing entanglement [28]. CM5 and CM4 exhibited optimal viscosity, supporting extended skin residence time and local bioavailability. This finding aligns with previous reports that polymer–lipid hybrids enable interfacial stabilization and controlled diffusion of hydrophobic phytochemicals. Moreover, the reduced spreadability and increased viscosity observed in some CM-SRMs are advantageous for topical delivery, as moderately viscous systems improve skin retention and reduce runoff after application.

Furthermore, pH has been shown to influence the stability and solubility of pharmaceutical preparations [29]. An acidic topical preparation enhances absorption but causes skin irritation, while an alkaline one prevents skin irritation but reduces absorption and spreadability. The pH stability study of the CM.SRMs as presented in Fig. 2C. were within the ranges 6.53 ± 0.02–7.21 ± 0.05 after the formulation. The pH of the formulation was relatively within the acceptable human skin pH of 4.5–6.5, suggesting minimal risk of irritation upon application [29]. There was an insignificant shift in the pH with time towards acidity of the SRMs, since these changes were minimal and formulation-dependent. This is minimal and will not affect the therapeutic activity of CM loaded in the SRMs. Stability in pH is an indication of stable formulations. In contrast, CM3 exhibited a small but significant decrease between day 7 and day 15 ($p < 0.05$), while CM5 showed a more pronounced early decrease in pH ($p < 0.05$), suggesting a slightly different matrix reorganization behavior in lipid-rich systems. Despite these significant differences, the absolute changes in pH were minimal and within a narrow physiological range, indicating that they are unlikely to affect formulation performance or induce skin irritation. Additionally, comparisons across formulations showed that CM1 and CM6 maintained comparable pH values at all points ($p > 0.05$), supporting the stability of the base matrix. CM5, on the other hand, differed consistently from other formulations ($p < 0.05$), likely

due to its higher lipid content. Overall, the observed pH stability supports the compatibility of CM with PEG-lipid matrix and indicates the absence of significant degradation or chemical instability during storage. The physicochemical trends are consistent with the structural organization of polymer-lipid hybrid systems, where the lipid phase contributes to matrix rigidity and drug retention, while PEG enhances hydration and flexibility [16].

3.3.2 FTIR, DSC, SEM, and DLS of CM.SRMs

To further elucidate the structural and molecular organization of the SRMs, representative formulations were analyzed using FTIR, DSC, SEM and DLS. The FTIR analysis focuses on identifying functional groups and observing any structural interactions that indicate complexation. FTIR spectrum of the CM (Fig. 3A) showed notable peaks at 2851.4–2922.2, 1707.1–1740.7, 1613.9–1651.2, 1401.1, and 1174.1–1275.4 cm^{-1}, which are characteristic of C–H stretching vibrations in aliphatic $–CH_2$ groups, C=O stretch typically found in esters or ketones, C=C of alkenes, carboxylate, and C-O stretching vibrations likely from alcohols, ethers, or glycosidic components, which are consistent with the presence of lipophilic and oxygenated phytoconstituents.

FTIR spectra of CM-SRMs exhibited no additional peaks compared to those of pure CM, blank SRMs, and individual excipients, indicating that no new chemical bonds or functional groups were formed during SRM formulation (Fig. 3A). However, slight band shifts and broadening, particularly in the O–H stretching region (around 3386–3242 cm^{-1}), were observed, suggesting non-covalent interactions such as hydrogen bonding within the PEG-lipid matrix. These interactions likely contribute to the physical incorporation of CM rather than chemical modification.

DSC analysis provided additional insight into the thermal behavior of the system. Differential scanning calorimetry (DSC) was carried out to determine the thermal behavior and compatibility of the components used in the SRM formulations. *Calopogonium mucunoides* (CM) exhibited a sharp endothermic peak at approximately 54.8°C in the DSC thermogram, which can be attributed to the melting of semi-crystalline phytoconstituents present in the crude extract, such as long-chain hydrocarbons, fatty acids, or waxy components [30]. This transition was significantly attenuated after incorporation of CM into the SRMs, with the heat flow profile of the loaded formulation (CM4) closely resembling that of the blank SRMs (CM6) (Fig. 3B). The reduction or disappearance of the CM-specific endothermic peak suggests that the extract is no longer present as a distinct crystalline phase but is dispersed within the PEG-lipid matrix. This behavior is consistent with reduced crystallinity and improved miscibility of the extract within the carrier system. Furthermore, the broad, sloping thermogram observed for glycerin reflects its amorphous and hygroscopic nature, indicating its role as a plasticizer that enhances molecular mobility and contributes to reduced structural order within the matrix. The observed thermal changes support partial loss of crystallinity and effective incorporation of CM within the SRM system. The morphological and structural properties of the CM-SRMs were further analyzed using SEM. SEM analysis revealed the formation of disrupted, amorphous SRM structures upon drug incorporation (Fig. 3C). The morphological and structural properties of the CM-SRMs were further analyzed using SEM. SEM analysis revealed the formation of disrupted, amorphous SRM structures upon drug incorporation (Fig. 3C). The unloaded matrix (CM6) exhibited a relatively organized, porous and vesicle-like architecture, indicative of a structured PEG-lipid network suitable for drug loading. In contrast, CM-loaded formulations (CM4) showed a more irregular and less ordered morphology, characterized by disrupted domains and non-uniform surfaces. This structural transition from an organized to a disordered system suggests successful incorporation of CM into the lipid matrix and a reduction in structural order. The crystalline, fibrous morphology observed in the raw CM further supports this interpretation, as these features were no longer evident after formulation. The observed morphological changes are consistent with the reduced crystallinity indicated by DSC and the non-covalent interactions

suggested by FTIR. Although SEM provides qualitative insight, the combined physicochemical and structural analyses collectively support effective dispersion of CM within the PEG-lipid matrix, with implications for improved stability and controlled topical delivery.

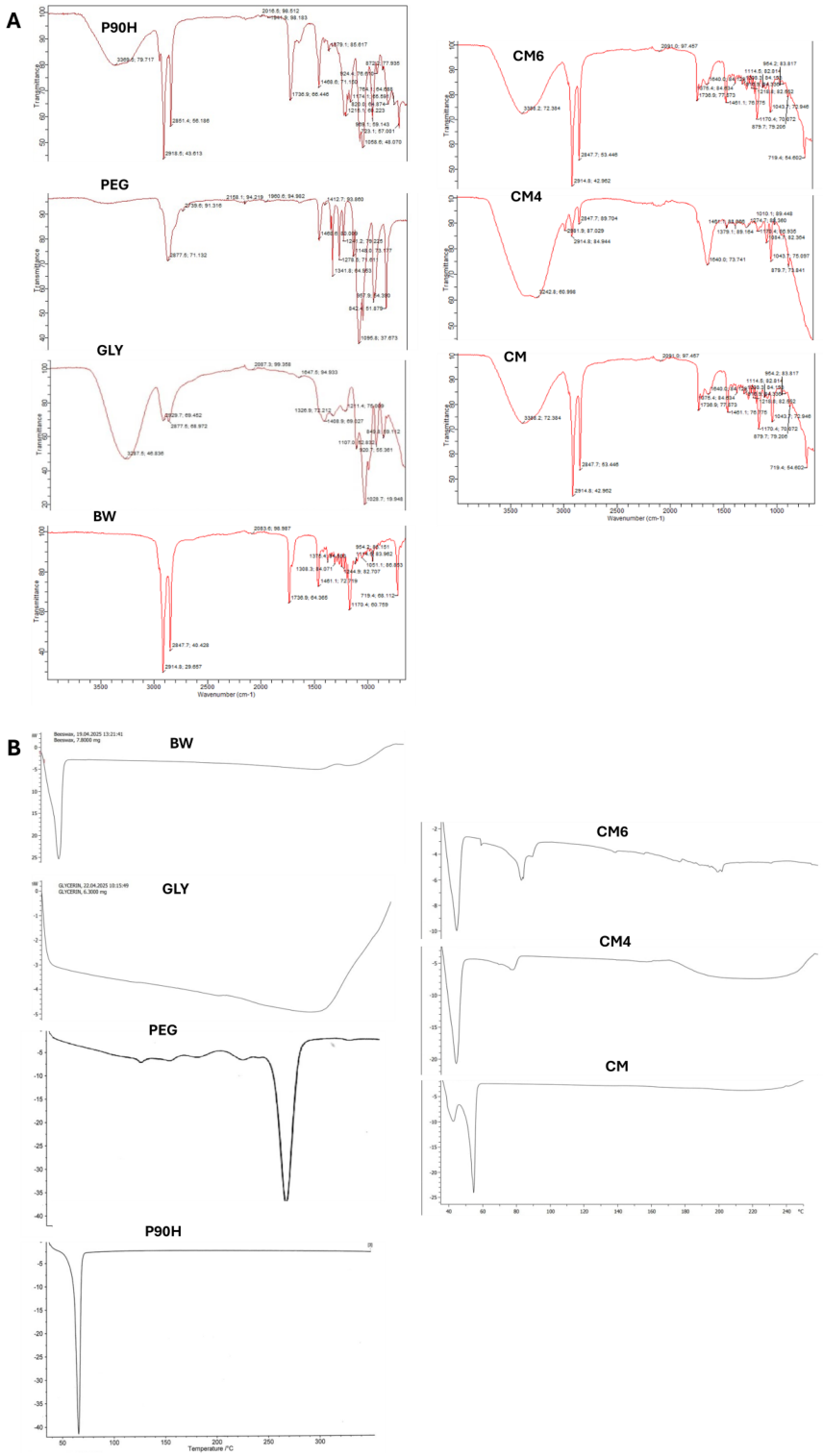

Figure 3: (Continued)

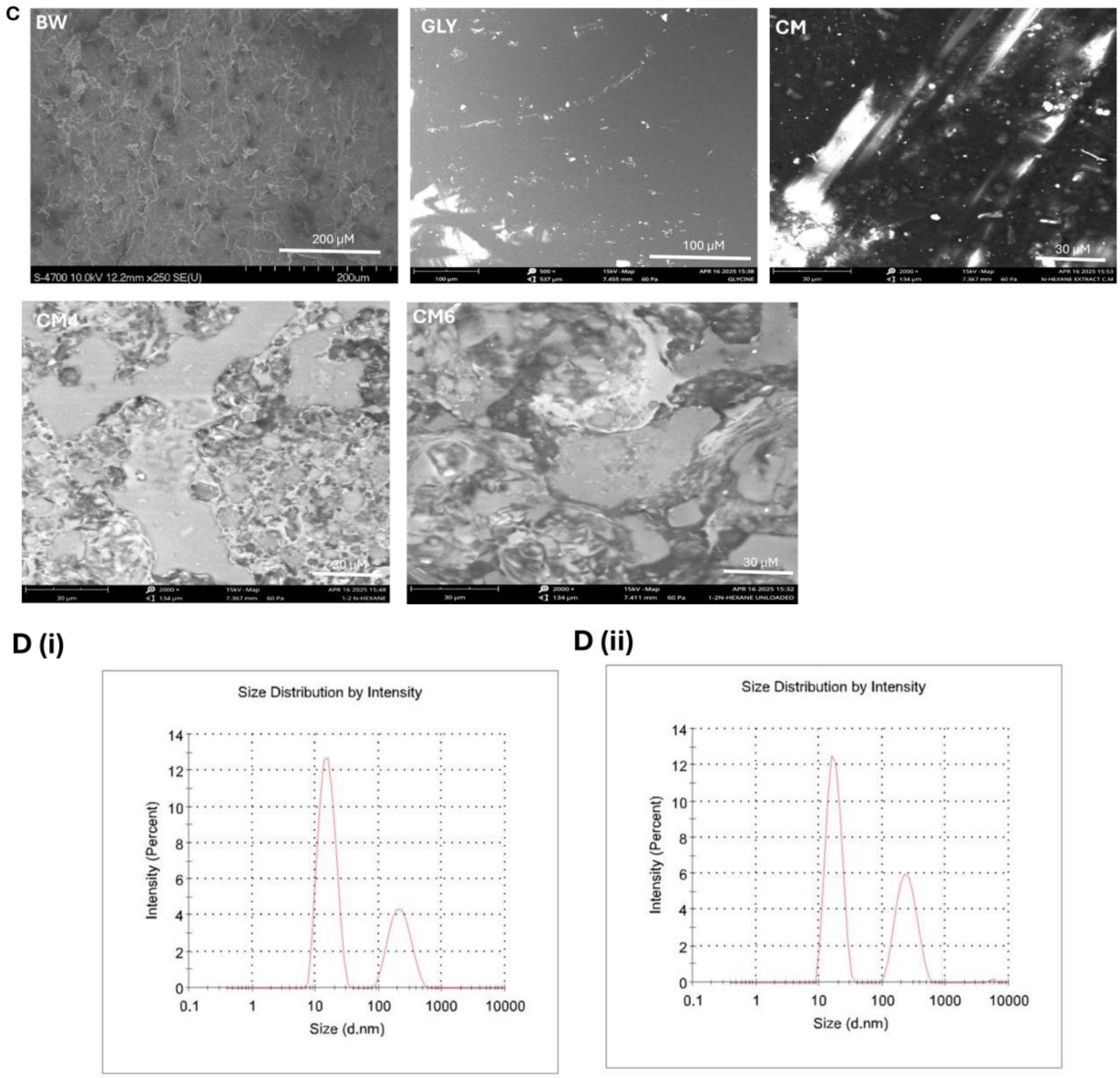

Figure 3: Physicochemical characterization of representative SRMs and excipients. (**A**) FTIR spectra of P90H, PEG 6000, glycerin, beeswax, CM6, CM4, and CM (**B**) DSC thermograms of beeswax, glycerin, PEG 6000, CM6, CM4, and CM (**C**) morphological and structural analysis of beeswax, glycerin, CM, CM4, CM6 conducted using SEM (**D**) particle size distribution of CM (i) and PEGylated SRM (CM4) (ii). P90H: phospholipon 90H, PEG 6000: polyethylene glycol 6000, CM4 correspond to PEG: lipid matrix (LM) ratio 1:2, while CM6 is the blank formulation without drug.

The particle size distribution of the pure extract and PEGylated SRM formulation (CM4; 1:2) was analyzed by dynamic light scattering. The pure extract exhibited a Z-average diameter of 20.63 nm with a PDI of 0.405, indicating moderate dispersion homogeneity. The intensity-based distribution revealed a bimodal profile, with a dominant population at approximately 15.68 nm and a secondary population around 224.5 nm, suggesting the presence of both nanoscale particles and larger aggregates. In contrast, the CM4 formulation showed a Z-average diameter of 27.02 nm with a higher PDI of 0.584, indicating a broader and more heterogeneous size distribution. The intensity-based distribution of CM4 also exhibited a bimodal

pattern, with populations in the ~10–20 and ~100–300 nm ranges, reflecting the coexistence of smaller micellar domains and larger aggregated structures (Fig. 3D). This increased heterogeneity in CM4 likely reflects the structural complexity of the polymer–lipid matrix and may contribute to the diffusion-controlled and sustained release behavior observed in the SRM system.

3.4 In Vitro Release Study and Release Kinetics of CM.SRMs

The *in vitro* release profiles of CM from the PEGylated SRM formulations of *Calopogonium mucunoides* (CM.SRMs) showed an initial release phase in simulated acidic fluid (SAF) (Fig. 4A) followed by continued release in simulated wound microenvironment fluid (SMF) (Fig. 4B), with release extent strongly dependent on polymer-lipid composition. The highest CM release of 90%, 48%, 90%, 80%, and 68% for CM1–CM5, respectively, in SMF (pH 6.8) over a 6-h period were obtained. After 5 min of incubation, there were significant differences in the release behavior across the formulations ($p < 0.05$) with CM1 consistently exhibiting the highest release and CM5 the lowest. Notably, as incubation time progressed, the release behavior of CM2 and CM3 became similar, with no significant differences, suggesting convergence of release profiles of moderate polymer-lipid ratios. The release behaviors of the formulations followed a similar but more pronounced trend in SMF (Fig. 4B). Overall, CM1 and CM3 exhibited relatively the fastest and highest release over time, whereas CM2 and CM5 showed slower release profiles. The rapid release from CM1 is attributable to the predominance of PEG and the absence of a lipid matrix, which favors hydration and diffusion. In contrast, the CM2 (SRMs containing PEG: LM 0:1) formulation, and CM5 (SRMs containing PEG: LM 1:3) showed significantly lower cumulative release, reaching just 48% and 68% over the study period compared to PEG-rich formulations. This may be attributed to a higher concentration of lipid matrix (LM) in the formulations, forming more compact hydrophobic and denser matrices that restrict medium penetration and drug diffusion, causing more prolonged release characteristics due to a reduction in matrix hydration and pore formation. Consequently, the compaction and lower porosity in the matrix resulted in delaying drug diffusion. This demonstrated that the PEG: lipid ratio plays a pivotal role in modulating CM release behavior from CM.SRMs which offers the potential for tailoring release profiles based on therapeutic requirements. Thus, PEG-rich systems favor rapid release and lipid-rich systems promote sustained release. This is consistent with a previous report [7]. Formulations CM3 (90%) and CM4 (80%) (containing PEG: LM 1:1 and 1:2, respectively) displayed intermediate release profiles. These outcomes suggest a synergistic balance between PEG's hydrophilic characteristics and the lipid matrix's ability to modulate drug encapsulation and release. The CM3 formulation exhibited greater structural stability. The CM5 characterized by the highest lipid content, demonstrated the slowest drug release among the PEG-containing formulations, with approximately 68% cumulative release at the end of the 6 h experiment. This slower release, when correlated with its maximum encapsulation efficiency (77%), indicated a denser and more hydrophobic matrix, which was effective at retaining and sustaining the drug (CM) with limiting diffusion. This tunable release profile highlights the potential of PEGylated SRMs as a versatile platform for controlled delivery of lipophilic plant extracts. The use of SMF of pH of 6.8 was to simulate the wound microenvironment (pH, 6–7) and also provides insight into the pH-responsive and matrix-dependent release characteristics of the formulations under standardized conditions.

In-vitro release data obtained in SAF and SMF were fitted to zero-order, first-order, Higuchi, and Korsmeyer-Peppas models to determine the release mechanism of CM from the PEGylated SRMs. The best-fit model was selected based on the highest correlation coefficient (R^2) [31]. In SAF, release behavior varied with formulation composition. CM2 and CM3 showed the best fit to the Higuchi model ($R^2 \approx 0.97$–0.98), indicating diffusion-controlled release. CM4 and CM5 followed first-order kinetics (R^2 up to 0.98), which suggests concentration-dependent release from a denser lipid matrix. CM1 was best described by

the Korsmeyer-Peppas model ($R^2 \approx 0.99$) with an n value (~0.92) indicative of anomalous (non-Fickian) transport (Supplementary Table S3A). In SMF (Supplementary Table S3B), release was more uniform, with the Higuchi model providing the best fit for CM2–CM5 ($R^2 \approx 0.97$–0.99). This confirms diffusion-controlled release. The Korsmeyer-Peppas model yielded n values <0.45 for CM3–CM5, indicating Fickian diffusion. CM1 showed weaker model fitting due to its rapid release profile. Overall, CM release was governed by polymer-lipid interactions, with PEG-rich systems favoring rapid release and lipid-rich formulations promoting sustained, diffusion-controlled release.

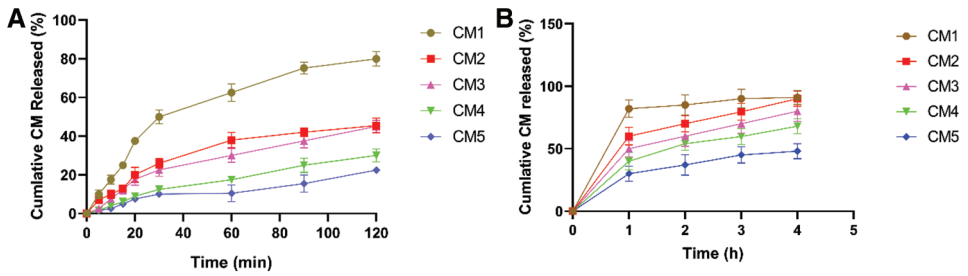

Figure 4: *In vitro* release profile of CM-SRMs in (**A**) simulated wound microenvironment (SWM; pH 6.8) and (**B**) simulated acidic fluid (SAF; pH 1.2). Data are presented as mean ± SD (n = 5). Statistical analysis was performed using two-way ANOVA followed by Tukey's multiple comparisons test ($p < 0.05$). CM1: PEG only (1:0); CM2, CM3, CM4, and CM5 correspond to PEG: lipid matrix (LM) ratios of 0:1, 1:1, 1:2, and 1:3, respectively.

3.5 Wound Size Reduction

The excision wound healing study conducted was to evaluate the effectiveness of CM in CM.SRMs (Group A) in the treatment of wounds, compared to the references: positive standard antibiotic (Group B), placebo (Group C), and untreated (Group D). Wound sizes measured on Days 0, 3, 7, 14, and 21, as shown in Fig. 5, showed that all groups displayed similar wound sizes on Day 0 (~2.0 cm), confirming consistent wound induction. Wound contraction was observed in Groups A and B on Day 3 post-treatment, with the wound size decreasing from 2.0 ± 0.11 to 1.6 ± 0.01 cm (20% wound contraction) and 1.8 ± 0.02 cm (10% wound contraction), respectively, indicating the onset of healing and the importance of antimicrobial activity in wound regeneration. Groups C (placebo) and D (untreated) also experienced a reduction to 1.9 ± 0.22 cm (5% wound contraction), but less remarkably, suggesting a delayed healing response. By Day 7 post-treatment, wounds in Groups A and B showed a higher wound size reduction of 0.7 ± 0.01 cm (65% wound contraction). On the same day, wounds in Groups C and D showed gradual healing, with sizes decreasing within the range 1.2 ± 0.12–1.4 ± 0.23 cm. Group C (placebo) wounds measured 1.0–1.4 cm, indicating only slight progression of healing in these groups. On day 21 post-treatment, a total and significant ($p < 0.05$) wound contraction with an epithelial growth was observed in group A (treated with CM.SRMs), demonstrating accelerated healing attributed to the bioavailability and improved skin penetration of the CM-based SRMs. This is likely due to the enhanced penetration/local availability, antimicrobial, and sustained release properties of the CM.SRMs. Moreover, it was observed that Group C (placebo) showed healing activity, which may be due to the constituents of the SRMs that delivered the CM. To enhance wound healing, the presence of an antimicrobial agent is important to prevent contamination and gangrene formation, which was synergistically supplied by CM and beeswax. Moreso, the presence of moisture is necessary on the wound surface to enable cell multiplication and migration that attracts speedy healing, which was encouraged by glycerin and PEG (that equally enhances and modulates surface charges, and good mucopenetrability. The moderate healing observed in the placebo group suggests a supportive contribution of the formulation base. However, the significantly greater contraction in Group A indicates an additional pharmacological effect of

the incorporated extract. The progressive and significant reduction in wound size over time further supports the effectiveness of the CM-SRM system in accelerating wound repair.

Thus, the goal of the present study was to ascertain the wound healing efficacy of CM-SRMs and support the therapeutic relevance of *Calopogonium mucunoides* in traditional medicine. While these findings demonstrate promising activity, the evaluation is limited to macroscopic wound contraction.

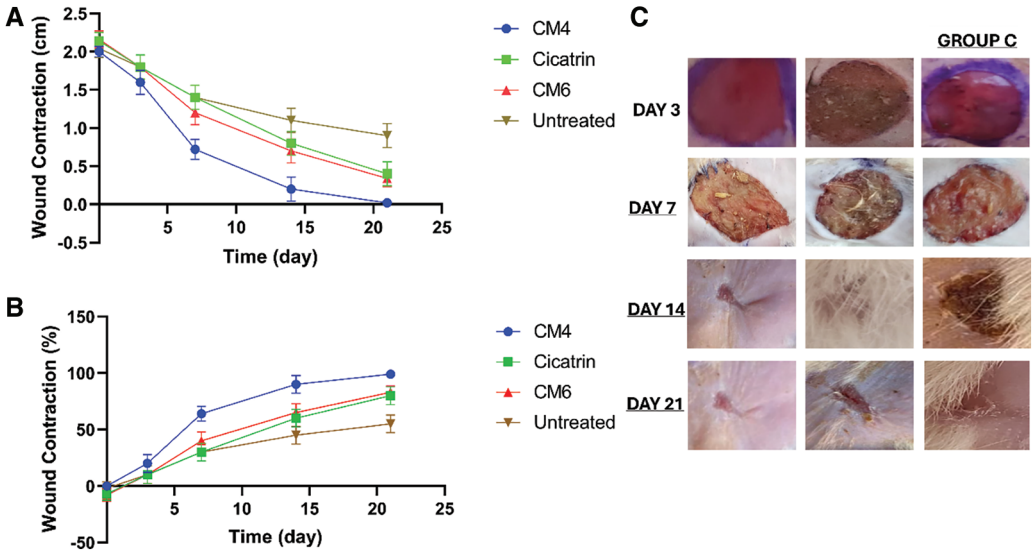

Figure 5: Wound healing activity of CM-SRMs in albino rats. (**A**). Wound contraction following treatment with CM4, cicatrin, and CM6 compared with that of the control. CM4, cicatrin, and CM6 were treated at a dosage of 5 mg/kg BW. (**B**) percentage wound contraction of treatment groups compared to control (**C**) Gross morphological representation of different treatment groups and control following treatment. Data are presented as mean ± SD (n = 5). Statistical analysis was performed using two-way ANOVA followed by Tukey's multiple comparisons test ($p < 0.05$). CM4 corresponds to a PEG: lipid matrix (LM) ratio of 1:2, while CM6 is the blank formulation without drug.

4 Conclusion

This research demonstrated a novel PEGylated *Calopogonium mucunoides*-based solid reverse micelle suspension (CM.SRMs) designed for wound application. The PEG: lipid matrix ratio was systematically varied to examine its influence on encapsulation efficiency, rheological behavior, structural organization, and release profile, thereby demonstrating the importance of polymer matrix interactions in modulating formulation performance. CM.SRMs exhibited characteristic prolonged and sustained properties, with improved bioavailability and significant wound healing. The SRMs notably enhance the stability of bioactive compounds, addressing key limitations such as poor bioavailability and rapid degradation. PEGylation improved drug spreadability, while the lipid matrix extended the sustained effect due to the three-dimensional network structure of carefully chosen excipients. Accelerated wound healing was observed with the drug-loaded SRMs ($p < 0.05$), unlike other formulations (references). The superior performance of this formulation highlights the potential of SRM technology in boosting the therapeutic effectiveness of traditional herbal remedies. Formulations CM4 and CM5 offered optimal structural properties, resulting in better therapeutic outcomes, including significantly increased wound contraction and epithelialization ($p < 0.05$) compared to standard treatment based on excision wound technique. These findings emphasize the synergistic role of PEGylation and lipid structuring in maintaining the bioavailability of plant-derived lipophilic actives at the wound site. Overall, PEGylated polymer–lipid SRMs are a promising hybrid delivery platform that combines

materials science design with practical wound-care benefits, supporting their potential use as an affordable and scalable technology for wound management, especially in resource-limited healthcare settings.

Although these findings are promising, the present study is limited by the use of UV-Vis quantification for a crude extract, the absence of histological and biomarker-based validation, and the lack of comparison with other advanced topical delivery systems. Future studies will therefore focus on validated analytical quantification, mechanistic wound-healing assays, evaluation in wound-relevant release media, and comparative assessment against other contemporary lipid-based formulations. Thus, *Calopogonium mucunoides*-based solidified reverse micellar suspensions could be a promising sustainable approach for wound management.

Acknowledgement: The authors acknowledged the technical assistance received from Ahmadu Bello University (ABU), Zaria, for thermal analyses and all the technical staff of Pharmaceutical Technology and Industrial Pharmacy.

Funding Statement: The authors received no specific funding for this study.

Author Contributions: The authors confirm contribution to the paper as follows: Conceptualization, Godswill C. Onunkwo, Edith O. Diovu, Eunice N. Anaele and Calister E. Ugwu; methodology, Iheanacho O. Enyum and Kingsley C. Eze; formal analysis, Samuel WisdomofGod Uzondu, Ogochukwu N. Umeh and Calister E. Ugwu; investigation, Iheanacho O. Enyum and Kingsley C. Eze; resources, Anthony A. Attama, Samuel WisdomofGod Uzondu and Calister E. Ugwu; data curation, Calister E. Ugwu and Eunice N. Anaele; writing—original draft, Calister E. Ugwu; writing review and editing, Godswill C. Onunkwo and Anthony Attama; visualization, Eunice N. Anaele and Ogochukwu N. Umeh; supervision, Calister E. Ugwu; project administration, Iheanacho O. Enyum, Kingsley C. Eze, Samuel WisdomofGod Uzondu, Ogochukwu N. Umeh and Calister E. Ugwu; fund acquisition, all authors. All authors reviewed and approved the final version of the manuscript.

Availability of Data and Materials: The data that support the findings of this study are available from the corresponding author upon reasonable request.

Ethics Approval: Experimental animal protocols were conducted according to the guidelines for conducting experiments stipulated and approved by our Institution's Animal Ethics Committee of Faculty of Pharmaceutical Sciences Research Ethics (approval No. FPSRE/UNN/25/00044) and in compliance with the Federation of European Laboratory Animal Science Associations and the European Union Directive 2010/63/EU for animal experiments.

Conflicts of Interest: The authors declare no conflicts of interest.

Supplementary Materials: The supplementary material is available online at https://www.techscience.com/doi/10.32604/jpm.2026.077511/s1.

References

1. Dasari N, Jiang A, Skochdopole A, Chung J, Reece EM, Vorstenbosch J, et al. Updates in diabetic wound healing, inflammation, and scarring. Semin Plast Surg. 2021;35(3):153–8. doi:10.1055/s-0041-1731460.
2. Nayak M, Banerjee D, Venugopal V, Nethi SK, Barui AK, Mukherjee S. Cell-engineered technologies for wound healing and tissue regeneration. npj Biomed Innov. 2025;2(1):38. doi:10.1038/s44385-025-00042-w.
3. Chitca DD, Popescu V, Mastalier B, Busu C. The economic burden of chronic wounds on global healthcare systems. Proc Int Conf Bus Excell. 2025;19(1):1995–2002. doi:10.2478/picbe-2025-0155.
4. Al Mamun A, Shao C, Geng P, Wang S, Xiao J. Recent advances in molecular mechanisms of skin wound healing and its treatments. Front Immunol. 2024;15:1395479. doi:10.3389/fimmu.2024.1395479.
5. Kumari P, Kant V, Chandratre GA, Ahuja M. Formulation and evaluation of pluronic F-127 thermoresponsive nanogels containing juglone for *in vivo* wound healing potential. BioNanoScience. 2024;14(5):4710–32. doi:10.1007/s12668-024-01429-6.

6. Rahmoun N, Boucherit-Otmani Z, Boucherit K, Benabdallah M, Choukchou-Braham N. Antifungal activity of the Algerian *Lawsonia inermis* (henna). Pharm Biol. 2013;51(1):131–5. doi:10.3109/13880209.2012.715166.
7. Akombaetwa N, Ilangala AB, Thom L, Memvanga PB, Witika BA, Buya AB. Current advances in lipid nanosystems intended for topical and transdermal drug delivery applications. Pharmaceutics. 2023;15(2):656. doi:10.3390/pharmaceutics15020656.
8. Enechi OC, Abugu M. Antidiarrheal and antibacterial activities of *Calopogonium mucunoides* Desv Leaf extracts. Global Veterinaria. 2016;16(2):155–64.
9. Egele ME, Enechi OC, Amah CC, Iyidiegwu FC, Okoro IJ, Amadi EB. Investigation of the anti-inflammatory activity and nutritional value of the leaves of *Calopogonium mucunoides*. Life Res. 2025;8(4):21. doi:10.53388/lr20250021.
10. Enechi OC, Odo CE, Okafor C. Assessment of the anti-ulcer action of the leaves of calopo (*Calopogonium mucunoides* Desv) in Wistar rats. J Pharm Res. 2014;8(1):24–7.
11. Sahle FF, Gebre-Mariam T, Dobner B, Wohlrab J, Neubert RHH. Skin diseases associated with the depletion of stratum corneum lipids and stratum corneum lipid substitution therapy. Skin Pharmacol Physiol. 2015;28(1):42–55. doi:10.1159/000360009.
12. Liu Y, Liang Y, Jing Y, Xin P, Han JL, Du Y, et al. Advances in nanotechnology for enhancing the solubility and bioavailability of poorly soluble drugs. Drug Des Dev Ther. 2024;18:1469–95. doi:10.2147/dDDT.s447496.
13. Momoh MA, Ossai EC, Chidozie OE, Precscila OO, Kenechukwu FC, Ofokansi KO, et al. A new lipid-based oral delivery system of erythromycin for prolong sustain release activity. Mater Sci Eng C. 2019;97(8):245–53. doi:10.1016/j.msec.2018.12.041.
14. Diab RF, Abdelghany TM, Gad S, Elbakry AM. Novel resveratrol smart lipids; design, formulation, and biological evaluation of anticancer activity. J Pharm Pharmacol. 2024;76(6):631–45. doi:10.1093/jpp/rgae009.
15. Uronnachi EM, Attama A, Kenechukwu F, Umeyor C, Gugu T, Nwakile C, et al. Solidified reverse micellar solution-(SRMS-) based microparticles for enhanced oral bioavailability and systemic antifungal efficacy of miconazole nitrate in immunocompromised mice. BioMed Res Int. 2022;2022(1):8930709. doi:10.1155/2022/8930709.
16. Ugwu CE, Oraeluno JN, Eze KC, Ezenma CO, Nwankwo AO. PEGylated aceclofenac solid lipid microparticles homolipid-based solidified reverse micellar solutions for drug delivery. Heliyon. 2022;8(4):e09247. doi:10.1016/j.heliyon.2022.e09247.
17. Eze KC, Ugwu CE, Odo FS, Njoku GC. Development and formulation of antidiabetic property of *Anarcadium occidantale*-based solid lipid microparticles. J Microencapsul. 2022;39(7–8):626–37. doi:10.1080/02652048.2022.2149967.
18. Ugwu C, Ugwoke C, Enyum I. Phytolipid delivery of *Pentaclethra macrophylla* (Fabaceae) extract: *in vitro* and *in vivo* activities. Trop J Pharm Res. 2025;24(7):881–8. doi:10.4314/tjpr.v24i7.4.
19. da Silva Favero J, dos Santos V, Weiss-Angeli V, Garcia CSC, Magnano GC, Henriques JAP, et al. Physicochemical characterization and safety assessment of cosmetic gels and emulsions containing sand-extraction clays. J Cosmet Dermatol. 2025;24(10):e70517. doi:10.1111/jocd.70517.
20. Agubata CO, Okereke C, Nzekwe IT, Onoja RI, Obitte NC. Development and evaluation of wound healing hydrogels based on a quinolone, hydroxypropyl methylcellulose and biodegradable microfibres. Eur J Pharm Sci. 2016;89(7 Suppl.):1–10. doi:10.1016/j.ejps.2016.04.017.
21. Patel S, Jadav M, Sammal D, Kulhari H, Pooja D. Liposomes-based delivery of phytoconstituents. In: Singh A, Kulhari H, Saharan VA, editors. Formulating pharma-, nutra-, and cosmeceutical products from herbal substances. Hoboken, NJ, USA: John Wiley & Sons, Inc.; 2025. doi:10.1002/9781119769484.ch15.
22. Jomova K, Alomar SY, Valko R, Liska J, Nepovimova E, Kuca K, et al. Flavonoids and their role in oxidative stress, inflammation, and human diseases. Chem Biol Interact. 2025;413(1):111489. doi:10.1016/j.cbi.2025.111489.
23. Shakil Shaikh S. Saponins and skin regeneration—a natural path to healing: harnessing plant-based bioactives for enhanced skin healing and renewal. Afr J Med Pharma Res. 2026;3(2):73–82. doi:10.18231/j.ajmpr.35030.1767590642.
24. Mehnert W. Solid lipid nanoparticles production, characterization and applications. Adv Drug Deliv Rev. 2001;47(2–3):165–96. doi:10.1016/s0169-409x(01)00105-3.

25. Joshi M, Butola BS, Saha K. Advances in topical drug delivery system: micro to nanofibrous structures. J Nanosci Nanotech. 2014;14(1):853–67. doi:10.1166/jnn.2014.9083.
26. Pardeike J, Hommoss A, Müller RH. Lipid nanoparticles (SLN, NLC) in cosmetic and pharmaceutical dermal products. Int J Pharm. 2009;366(1–2):170–84. doi:10.1016/j.ijpharm.2008.10.003.
27. Ozkan G, Ugur ES, Capanoglu E. Ultrasonication-enabled liposomal encapsulation of *Propolis* extract: bioaccessibility, bioavailability, and food application. Food Bioprocess Technol. 2026;19(4):189. doi:10.1007/s11947-026-04205-4.
28. Lapenna A, Dagallier C, Huille S, Tribet C. Poly(glutamic acid)-based viscosity reducers for concentrated formulations of a monoclonal IgG antibody. Mol Pharmaceutics. 2024;21(2):982–91. doi:10.1021/acs.molpharmaceut.3c01159.
29. Rehman A, Iqbal M, Khan BA, Khan MK, Huwaimel B, Alshehri S, et al. Fabrication, *in vitro*, and *in vivo* assessment of eucalyptol-loaded nanoemulgel as a novel paradigm for wound healing. Pharmaceutics. 2022;14(9):1971. doi:10.3390/pharmaceutics14091971.
30. Lee EY, Choi J, Kim YM, Yang K, Jang AY, Shin HK, et al. Plant derived extract loaded nanostructured lipid carriers with enhanced oral delivery for the treatment of acute inflammation. Sci Rep. 2025;15(1):34551. doi:10.1038/s41598-025-17898-y.
31. Balu P, Srikanth S, Gnandhas DP, Durai RD, Ulaganathan V, Narayanan B, et al. Development and optimization of an injectable *in-situ* gel system for sustained release of anti-tuberculosis drugs. Sci Rep. 2025;15(1):21383. doi:10.1038/s41598-025-05644-3.